Thermal transport through a mesoscopic weak link

Kelly R. Patton and Michael R. Geller
Department of Physics and Astronomy, University of Georgia, Athens, Georgia 30602-2451
(January 4, 2001)

We calculate the rate of energy flow between two macroscopic bodies, each in thermodynamic equilibrium at a different temperature, and joined by a weak mechanical link. The macroscopic solids are assumed to be electrically insulating, so that thermal energy is carried only by phonons. To leading order in the strength of the weak link, modeled here by a harmonic spring, the thermal current is determined by a product of the local vibrational density-of-states of the two bodies at the points of connection. Our general expression for the thermal current can be regarded as a thermal analog of the well-known formula for the electrical current through a resistive barrier. It is also related to the thermal Landauer formula in the weak-tunneling limit. Implications for heat transport experiments on dielectric quantum point-contacts are discussed.

PACS: 63.22.+m, 66.70.+f, 68.65.-k

I. INTRODUCTION

Mesoscopic phonon systems are relatively unexplored compared with their electronic counterparts. An exception is the recent work on thermal conductance quantization in freely suspended one-dimensional dielectric wires, where the thermal conductance was found to be $\pi k_{\rm B}^2 T/6\hbar$ per transmitted vibrational mode [1,2]. This behavior parallels the well known electrical conductance quantization in units of $e^2/2\pi\hbar$ per (spin-resolved) channel in one-dimensional mesoscopic conductors [3–5]. Electrical conductance quantization and many other aspects of mesoscopic transport in one-dimensional Fermi liquids, as well as edge-state transport in integral quantum Hall effect systems, can be understood with the Landauer and Landauer-Büttiker formalisms [5,6].

The conventional Landauer formula describes charge transport in mesoscopic conductors in the limit where there exists one or more propagating channels [7]. Another important transport regime is the weak tunneling limit, where the charge conductance is much less than $e^2/2\pi\hbar$ and, as shown by Schrieffer *et al.* [8,9], is determined by the density-of-states (DOS) obtained from the one-particle Green's function.

The thermal analog of the weak tunneling limit has not been addressed theoretically and is interesting for several reasons. First, a microscopic quantum description of thermal conduction through weak links is crucial for understanding energy dissipation in nanostructures such as nanoparticles, nanotubes, molecular circuits, and nanometer-scale electromechanical systems. As we shall demonstrate, the classical theory of thermal conduction, based on the heat equation, is entirely inapplicable to these systems. Second, thermal conduction through a weak link connected to a macroscopic solid turns out to be a sensitive local probe of the surface vibrational DOS of that solid, suggesting the possibility of a surface microscopy based on a scanning *thermal* probe.

In this paper we calculate the rate $I_{\rm th}$ of thermal energy flow between two macroscopic bodies, each in thermodynamic equilibrium, and joined by a weak mechanical link. The weak link may consist of one or more chemical bonds, or by a narrow "neck" of dielectric material, both of which can be accurately modeled by a harmonic spring of stiffness K. We obtain a general expression for the thermal current that can be regarded as a thermal analog of the well-known formula, derived by Schrieffer *et al.* [8], for the electrical current through a resistive barrier. Our result can also be interpreted as an application of the thermal Landauer formula [2,10] in the weak tunneling limit, with the energy-dependent phonon transmission probability calculated microscopically.

Our work is also related to the classic work of Little [11] on the thermal boundary resistance at an interface between two dielectrics, a solid-solid analog of the Kapitza resistance between solids and superfluid Helium caused by phonon scattering at the interface. A tunneling-Hamiltonian approach similar to ours has been applied to the Kapitza resistance problem by Sheard and Toombs [12]. In our geometry, however, the thermal resistance comes from scattering at the weak link, and the thermal current depends on the elastic properties of the link and does not vanish if the solids are identical. Heat transport in mesoscopic junctions has been studied recently with the scattering approach by Cross and Lifshitz [13]. Thermal transport through weak links has also been studied in conductors, including the two-dimensional electron gas [14,15] and one-dimensional Luttinger liquids [16].

The organization of our paper is as follows: In the next section we describe in detail our mesoscopic weak-link model, and in Section III we define and calculate the local vibrational DOS for the macroscopic solids. A general expression for the thermal current is derived in Section IV. Some experimental implications are discussed in Section V, where we calculate the thermal conductance through a nanometer-scale junction in Si. Section VI contains a discussion of the differences between electron and phonon tunneling, and also of the role of phonon phase

coherence in this work.

II. MESOSCOPIC WEAK LINK

The model we consider is as follows: Two macroscopic solids, L and R, are held at fixed temperatures $T_{\rm L}$ and $T_{\rm R}$. The two bodies are assumed to be electrically insulating, so that thermal energy is carried only by phonons. The Hamiltonian of the isolated solids is (we set $\hbar = 1$)

$$H_0 = H_{\rm L} + H_{\rm R}, \tag{1}$$

where

$$H_I \equiv \sum_n \omega_{In}\, a^\dagger_{In}\, a_{In}, \qquad I = {\rm L}, {\rm R}. \tag{2}$$

The $a^\dagger_{nI}$ and a_{nI} are phonon creation and annihilation operators for the left and right sides, satisfying

$$[a_{nI}, a^\dagger_{n'I'}] = \delta_{nn'}\,\delta_{II'} \tag{3}$$

and

$$[a_{nI}, a_{n'I'}] = [a^\dagger_{nI}, a^\dagger_{n'I'}] = 0. \tag{4}$$

The vibrational modes of the isolated bodies are labeled by n and have energies ω_{In}. Our analysis is valid for any ω_{In}. The mesoscopic weak-link model is illustrated in Fig. 1.

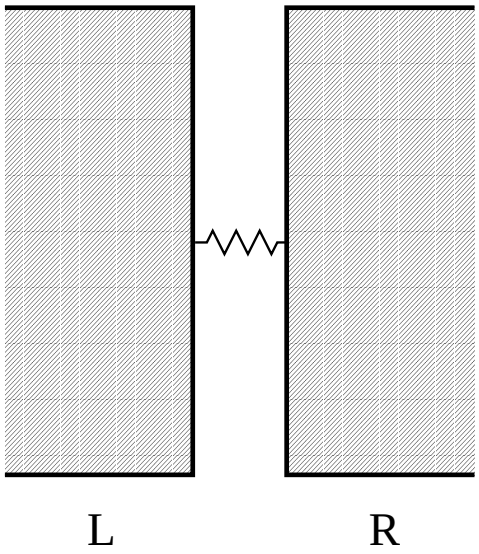

FIG. 1. Weak link model. Two macroscopic dielectrics, at temperatures $T_{\rm L}$ and $T_{\rm R}$, are joined by a harmonic spring of stiffness K.

The two macroscopic solids are connected by a weak mechanical link, which we model by a harmonic spring with stiffness K,

$$\delta H = \tfrac{1}{2} K \big(u^z_{\rm L} - u^z_{\rm R}\big)^2. \tag{5}$$

Here u^z_I is the normal component of the displacement field at the surface of body I at the point of connection to the weak link, with the surface normal taken to be in the z direction. The surface displacements can be expanded in a basis of phonon annihilation and creation operators as

$$u^z_I = \sum_n \big(h_{In} a_{In} + h^*_{In} a^\dagger_{In}\big), \qquad I = {\rm L}, {\rm R} \tag{6}$$

where the h_{In} are model-dependent complex coefficients. The h_{In} appropriate for the stress-free planar surface of a semi-infinite isotropic elastic continuum are given below.

As discussed above, we are interested in systems where the mechanical interaction between the two bodies is actually caused by one or more atomic bonds, or by a narrow "neck" of dielectric material. Our harmonic spring model correctly accounts for the longitudinal (normal to the surface) elastic forces between the solids, but neglects any transverse or torsional interaction. Although transverse and torsional forces can be included by a straightforward generalization of our model, they are often much smaller than the longitudinal coupling.

The macroscopic bodies act as thermal reservoirs, and are taken to be ideal thermal conductors. In particular, they are assumed to be harmonic [see Eq. (2)]. Therefore, the thermal resistance we calculate is caused entirely by the scattering of phonons at the junction between the reservoirs and the weak link, and by the finite transmission probability through the link.

III. LOCAL VIBRATIONAL DOS

In what follows we will need the *local* vibrational DOS (or, more precisely, local spectral density) of the bulk solids, evaluated at the point of contact with the weak link. These can be obtained from the retarded surface-displacement correlation functions

$$D_I(t) \equiv -i\theta(t)\big\langle [u^z_I(t), u^z_I(0)]\big\rangle_0 \tag{7}$$

for the isolated macroscopic bodies L and R. Using (6) leads to

$$D_I(t) = -2\,\theta(t) \sum_n |h_{In}|^2 \sin(\omega_{In} t). \tag{8}$$

The local DOS $N_I(\omega)$ is then defined in terms of the Fourier transform of (7),

$$N_I(\omega) \equiv -\tfrac{1}{\pi}\,{\rm Im}\, D_I(\omega). \tag{9}$$

Then we have

$$N_I(\omega) = \sum_n |h_{In}|^2 [\delta(\omega - \omega_{In}) - \delta(\omega + \omega_{In})]. \tag{10}$$

In many cases of interest the local spectral density is an algebraic function of energy at low energies,

$$N_I(\omega) \propto \omega^\alpha, \tag{11}$$

where α is a constant. For example, $\alpha = 1$ at the planar surface of a semi-infinite isotropic elastic continuum (see below).

IV. THERMAL CURRENT

We now calculate the heat flow between the two bodies joined by the weak link. The complete system is described by the Hamiltonian

$$H = H_0 + \delta H. \tag{12}$$

We define a thermal current operator $\hat{I}_{\rm th}$ according to

$$\hat{I}_{\rm th} \equiv \partial_t H_{\rm R} = i[H, H_{\rm R}]. \tag{13}$$

The expectation value of $\hat{I}_{\rm th}$ is the energy per unit time flowing from the left to the right body.

Writing the interaction (5) as

$$\delta H = \tfrac{1}{2} K \sum_{nn'} (A_{{\rm L}n} - A_{{\rm R}n})(A_{{\rm L}n'} - A_{{\rm R}n'}), \tag{14}$$

where

$$A_{In} \equiv h_{In}\, a_{In} + h^*_{In}\, a^\dagger_{In}, \tag{15}$$

we find that the thermal current operator then takes the form

$$\hat{I}_{\rm th} = \frac{iK}{2} \sum_{nn'} \omega_{{\rm R}n} \big\{ A_{{\rm R}n'} - A_{{\rm L}n'}, h_{{\rm R}n}\, a_{{\rm R}n} - h^*_{{\rm R}n}\, a^\dagger_{{\rm R}n} \big\}, \tag{16}$$

where $\{\cdot\,,\cdot\}$ is an anticommutator.

The equation of motion for the density matrix in the interaction representation is

$$\partial_t \rho(t) = i\big[\rho(t), \delta H(t)\big], \tag{17}$$

where

$$O(t) \equiv e^{iH_0 t} O e^{-iH_0 t}. \tag{18}$$

From (17) we find that the nonequilibrium thermal current to leading order is

$$I_{\rm th}(t) = i \int_0^t dt' \big\langle [\delta H(t'), \hat{I}_{\rm th}(t)] \big\rangle_0. \tag{19}$$

Evaluating Eq. (19) leads to our principal result (with factors of $\hbar$ reinstated)

$$I_{\rm th} = \frac{2\pi K^2}{\hbar} \int_0^\infty d\epsilon\, \epsilon\, N_{\rm L}(\epsilon)\, N_{\rm R}(\epsilon) \big[n_{\rm L}(\epsilon) - n_{\rm R}(\epsilon) \big]. \tag{20}$$

Here $n_{\rm L}(\epsilon)$ and $n_{\rm R}(\epsilon)$ are Bose distribution functions

$$n(\epsilon) \equiv 1 \big/ \big(e^{\epsilon/k_{\rm B}T} - 1 \big) \tag{21}$$

with temperatures $T_{\rm L}$ and $T_{\rm R}$. The details leading to Eq. (20) are given in Appendix A.

Our result (20) shows that the thermal current between a dielectric held at zero temperature and a second dielectric at temperature T will be a power-law function of T, in striking contrast with nonmesoscopic thermal transport. For example, assuming a spectral density of the form (11) leads at low temperature to

$$I_{\rm th} \propto T^{2\alpha+2}, \tag{22}$$

where T is the temperature of the second body.

The linear thermal conductance, defined by

$$G_{\rm th} \equiv \lim_{T_{\rm L} \to T_{\rm R}} \frac{I_{\rm th}}{T_{\rm L} - T_{\rm R}}, \tag{23}$$

is given by

$$G_{\rm th} = \frac{2\pi K^2}{\hbar} \int_0^\infty d\epsilon\, \epsilon\, N_{\rm L}(\epsilon)\, N_{\rm R}(\epsilon)\, \frac{\partial n(\epsilon)}{\partial T}. \tag{24}$$

This expression, along with Eq. (11), shows that the linear thermal conductance between two dielectrics held at a common temperature T, varies at low temperature as a power-law in T,

$$G_{\rm th} \propto T^{2\alpha+1}, \tag{25}$$

where α is the exponent characterizing the power-law spectral density at low energies.

V. THERMAL CONDUCTANCE OF NANOMETER-SCALE SILICON JUNCTION

In this section we give a simple application of our theory to a structure consisting of a cylindrical neck of Si material connecting two semi-infinite Si crystals. To be in the mesoscopic regime we assume the dimensions of the weak link to be smaller than the phase-coherence length of the phonons. The geometry of the system we consider is shown schematically in Fig. 2.

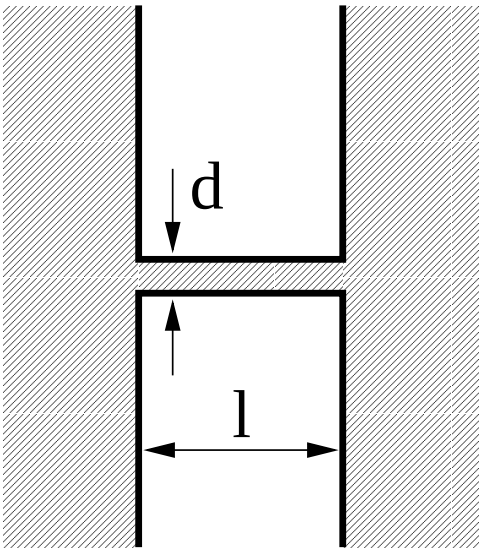

FIG. 2. Cylindrical silicon junction of length l and diameter d.

To apply our formula (24) we need the phonon spectral density at the surface of Si, and also the effective spring constant of the link. The spectral density at energies much less than the Debye energy may be obtained from elasticity theory. This approach, which requires a detailed consideration of the vibrational modes of a semi-infinite elastic continuum with a stress-free planar surface, is carried out in Appendix B. We show there that the spectral density at the surface of Si is

$$N(\epsilon) = C\epsilon, \qquad C \approx 1.3 \times 10^8 \text{ cm}^2 \text{ erg}^{-2}. \tag{26}$$

Then using (24) we obtain [17]

$$G_{\rm th} = (8\pi^5 K^2 C^2 k_{\rm B}^4/15\hbar)\, T^3. \tag{27}$$

The longitudinal stiffness of the mechanical link, a cylinder of length l and diameter d, is

$$K = \frac{\pi d^2}{4\,l}\, Y, \tag{28}$$

where Y is Young's modulus. For Si, [18]

$$Y \approx 1.3 \times 10^{12} \text{ dyn cm}^{-2}, \tag{29}$$

and assuming link dimensions of $l = 10\,\text{nm}$ and $d = 1\,\text{nm}$, we obtain

$$K \approx 1.0 \times 10^4 \text{ erg cm}^{-2}, \tag{30}$$

and a thermal conductance of

$$G_{\rm th} = (9.5 \times 10^{-11} \text{ erg s}^{-1} \text{ K}^{-4})\; T^3. \tag{31}$$

It is interesting to compare this result with the "classical" thermal conductance

$$G_{\rm th}^{\rm cl} = \frac{\pi d^2}{4\,l}\,\kappa \tag{32}$$

of the cylindrical link, as predicted by the heat equation. Here κ is the experimentally measured bulk thermal conductivity, itself a function of temperature, which for Si can be parameterized as [19]

$$\kappa = \frac{10^7 \text{ erg s}^{-1} \text{ cm}^{-1} \text{ K}^{-1}}{0.16 + 1.5\times10^{-3}\,T + 1.6\times10^{-6}\,T^2}, \tag{33}$$

with temperature in K. Eq. (33) is accurate down to about 100K, below which one can use the low-temperature data of Ref. [20].

In Fig. 3 we plot our result (31) along with the classical thermal conductance (32) of the same Si link. As is evident, these are dramatically different at low temperatures. The large difference occurs because, as discussed in Section VI, the origin of the thermal resistance in the two formulas (31) and (32) are different. Although it is tempting to conclude that they begin to agree at higher temperature, this would be incorrect, because our theory breaks down at higher temperature and Eq. (31) is not valid up to the temperature where the curves meet.

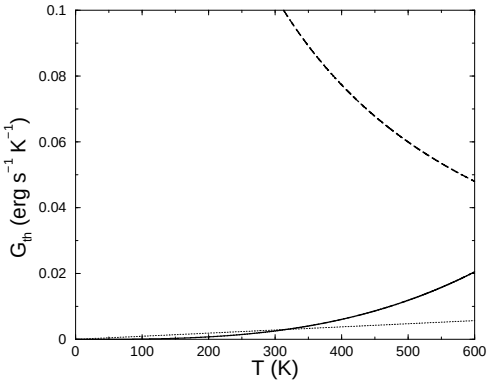

FIG. 3. Thermal conductance of the mesoscopic Si link shown in Fig. 2, as a function of temperature. The solid line follows from Eq. (31), and the dashed line from the corresponding classical result given in Eq. (32). The thin dotted line is the universal thermal conductance $\pi k_{\rm B}^2 T/6\hbar$ of a single propagating channel.

There are four reasons why our analysis becomes invalid as the temperature is increased: The first is that we have assumed the weak link to be of mesoscopic dimensions. As the temperature increases, anharmonic interaction will eventually make the phonon phase-coherence length smaller than the size of the link. While an estimate of the phase-coherence length is beyond the scope of this work, the experiment of Schwab *et al.* [1] suggests that in Si it is at least 1 nm at 1 K. The second is that our estimate of the spectral density is only valid for temperatures much less than the Debye temperature of Si, about 625 K. The third reason is that the leading-order perturbation theory we have used breaks down when $G_{\rm th}$ approaches the thermal conductance $\pi k_{\rm B}^2 T/6\hbar$ corresponding to one propagating channel, shown as a thin dotted

line in Fig. 3. And the fourth reason is that we have neglected any electronic contribution to $G_{\rm th}$, which is correct only when $k_{\rm B}T$ is much less than the Si band gap. Taking all of these factors into consideration suggests that Eq. (31) is probably not quantitatively correct beyond about 10 K.

VI. DISCUSSION

In this paper we have studied the thermal analog of the weak tunneling limit of charge conduction—which might be regarded as phonon "tunneling"—and find many similarities to electron tunneling. There are a few important differences, however.

Electron tunneling, as it is usually defined, involves the passage of an electron through a classically forbidden region. In the thermal case, a phonon of energy ϵ is never in a region that does support a mode at that energy. [21] For example, the harmonic spring employed in Eq. (5) can support a single propagating phonon channel, but phonons incident on the weak link are mostly reflected back into the macroscopic dielectrics. Whereas the tunneling rate of an electron (at a fixed energy ϵ) through a forbidden region of thickness l varies exponentially with l in the weak-tunneling limit, the thickness dependence in the phonon tunneling case is different. In the example discussed in Section V, the thermal conductance varies with length l of the bridge as l^{-2}, because the effective spring constant (28) of the bridge becomes softer with increasing l.

We have demonstrated that the classical theory of thermal conduction, based on the heat equation and on the concept of a local thermal conductivity, is entirely inapplicable to mesoscopic dielectrics. In a mesoscopic dielectric, thermal resistance is caused by elastic scattering of phonons, whereas in an infinite, disorder-free crystal it is caused by inelastic scattering due to anharmonicity. In the example of Section V, the quantum result (27) is determined by the *mechanical* properties of the bridge material, through the elastic modulus Y, whereas the classical result (32) is determined by the bridge material's bulk thermal conductivity κ.

ACKNOWLEDGMENTS

This work was supported by the Research Corporation. It is a pleasure to thank Steve Lewis for useful discussions.

APPENDIX A: GENERAL FORMULA FOR THE THERMAL CURRENT

Evaluating (19) we find

$$I_{\rm th}(t) = \frac{K^2}{2} \sum_{nn'mm'} \int_0^t dt'\ \omega_{{\rm R}n}\ {\rm Re}\ \Big\langle \Big\{ A_{{\rm L}m}(t') - A_{{\rm R}m}(t'), \Big[A_{{\rm L}m'}(t') - A_{{\rm R}m'}(t')\,, \Big(A_{{\rm L}n'}(t) - A_{{\rm R}n'}(t) \Big) \times \Big(h_{{\rm R}n}\, a_{{\rm R}n}(t) - h^*_{{\rm R}n}\, a^\dagger_{{\rm R}n}(t) \Big) \Big] \Big\} \Big\rangle_0 , \tag{A1}$$

and, after further simplification,

$$I_{\rm th}(t) = \frac{K^2}{2} \sum_{nn'} \int_0^t dt'\ \omega_{{\rm R}n}\ {\rm Re}\ \Big\langle \Big(\big\{ A_{{\rm L}n'}(t), A_{{\rm L}n'}(t') \big\} + \big\{ A_{{\rm R}n'}(t), A_{{\rm R}n'}(t') \big\} \Big) \Big[h_{{\rm R}n}\, a_{{\rm R}n}(t) - h^*_{{\rm R}n}\, a^\dagger_{{\rm R}n}(t),\ A_{{\rm R}n}(t') \Big] + \Big\{ h_{{\rm R}n}\, a_{{\rm R}n}(t) - h^*_{{\rm R}n}\, a^\dagger_{{\rm R}n}(t),\ A_{{\rm R}n}(t') \Big\} \Big(\big[A_{{\rm L}n'}(t), A_{{\rm L}n'}(t') \big] + \big[A_{{\rm R}n'}(t), A_{{\rm R}n'}(t') \big] \Big) \Big\rangle_0 , \tag{A2}$$

where we have used the fact that the commutators are c-numbers. The required thermal expectation values are

$$\big\langle \big\{ A_{In}(t), A_{In}(t') \big\} \big\rangle_0 = 2\,|h_{In}|^2 \left[1 + 2\,n_I(\omega_{In}) \right] \cos\omega_{In}(t-t'), \tag{A3}$$

$$\big\langle \big[A_{In}(t), A_{In}(t') \big] \big\rangle_0 = -2i\,|h_{In}|^2 \sin\omega_{In}(t-t'), \tag{A4}$$

$$\big\langle \big[h_{{\rm R}n}\, a_{{\rm R}n}(t) - h^*_{{\rm R}n}\, a^\dagger_{{\rm R}n}(t),\ A_{{\rm R}n}(t') \big] \big\rangle_0 = 2\,|h_{{\rm R}n}|^2 \cos\omega_{{\rm R}n}(t-t'), \tag{A5}$$

and

$$\big\langle \big\{ h_{{\rm R}n}\, a_{{\rm R}n}(t) - h^*_{{\rm R}n}\, a^\dagger_{{\rm R}n}(t),\ A_{{\rm R}n}(t') \big\} \big\rangle_0 = -2i\,|h_{{\rm R}n}|^2 \left[1 + 2\,n_{\rm R}(\omega_{{\rm R}n}) \right] \sin\omega_{{\rm R}n}(t-t'). \tag{A6}$$

These lead to

$$I_{\rm th}(t) = 2K^2 \sum_{nn'} \omega_{{\rm R}n}\ |h_{{\rm R}n}|^2\ \int_0^t dt' \big(\, |h_{{\rm L}n'}|^2 \big[1 + 2\, n_{\rm L}(\omega_{{\rm L}n'})\big] \cos\omega_{{\rm L}n'}(t-t')\ \cos\omega_{{\rm R}n}(t-t')$$
$$+\ |h_{{\rm R}n'}|^2 \big[1 + 2\, n_{\rm R}(\omega_{{\rm R}n'})\big] \cos\omega_{{\rm R}n}(t-t')\ \cos\omega_{{\rm R}n'}(t-t')$$
$$-\ |h_{{\rm L}n'}|^2 \big[1 + 2\, n_{\rm R}(\omega_{{\rm R}n})\big] \sin\omega_{{\rm L}n'}(t-t')\ \sin\omega_{{\rm R}n}(t-t')$$
$$-\ |h_{{\rm R}n'}|^2 \big[1 + 2\, n_{\rm R}(\omega_{{\rm R}n})\big] \sin\omega_{{\rm R}n}(t-t')\ \sin\omega_{{\rm R}n'}(t-t')\big). \tag{A7}$$

Here $n_{\rm L}(\epsilon)$ and $n_{\rm R}(\epsilon)$ are Bose distribution functions [see Eq. (21)] with temperatures $T_{\rm L}$ and $T_{\rm R}$. Next we make a change of variables $t' \to t - t'$, take the $t \to \infty$ limit, and include a convergence factor to regularize the long-time behavior of the resulting integrals. Finally, using the identities

$$\int_0^\infty dt\ \cos\omega t\ \cos\omega' t\ e^{-\zeta t} = \frac{\pi}{2}\big[\delta(\omega-\omega') + \delta(\omega+\omega')\big] \tag{A8}$$

and

$$\int_0^\infty dt\ \sin\omega t\ \sin\omega' t\ e^{-\zeta t} = \frac{\pi}{2}\big[\delta(\omega-\omega') - \delta(\omega+\omega')\big], \tag{A9}$$

where ζ is a positive infinitesimal, and reinstating factors of $\hbar$, leads to Eq. (20).

In Eqs. (20) and (24) we have introduced an *energy*-dependent DOS,

$$N_I(\epsilon) \equiv \sum_n |h_{In}|^2 [\delta(\epsilon - \hbar\omega_{In}) - \delta(\epsilon + \hbar\omega_{In})] \tag{A10}$$

which has dimensions of (length)^2/energy. In a homogeneous elastic continuum of mass density ρ and volume V, $N(\epsilon)$ is equal to $\hbar^2/2\rho\epsilon$ times the thermodynamic DOS per volume, $V^{-1}\sum_n \delta(\epsilon - \epsilon_n)$.

APPENDIX B: SURFACE DOS OF SILICON

In this appendix we calculate the local phonon DOS at the stress-free planar surface of a semi-infinite isotropic elastic continuum, following closely the work of Ezawa [22], and use this to estimate the DOS at the surface of Si. The substrate is assumed to occupy the space $z \ge 0$. The vibrational modes are labeled by $n = (m, \mathbf{K}, c)$, where m is a branch index taking the values SH, $\pm$, 0, and R, $\mathbf{K}$ is a two-dimensional wave vector in the xy plane, and $c \equiv \omega/|\mathbf{K}|$ is a parameter (continuous for all branches except $m = {\rm R}$) with dimensions of velocity. In contrast to Ref. [22] we shall use periodic boundary conditions in the x and y directions, over a square of area $\mathcal{A}$.

In our analysis we will approximate Si as an isotropic elastic continuum with longitudinal and transverse sound velocities

$$v_{\rm l} = 8.5 \times 10^5\,{\rm cm\ s^{-1}},$$
$$v_{\rm t} = 5.9 \times 10^5\,{\rm cm\ s^{-1}}, \tag{B1}$$

and mass density

$$\rho = 2.3\,{\rm g\ cm^{-3}}. \tag{B2}$$

It will be convenient to treat the Rayleigh branch ($m = {\rm R}$) separately, and then consider the branches with continuous c. In the Rayleigh case the displacement field is expanded as [23]

$$\mathbf{u} = \sum_{\mathbf{K}} \sqrt{\frac{\hbar}{2\rho c_{\rm R}|\mathbf{K}|}}\ \big[a_{{\rm R}\mathbf{K}}\, \mathbf{f}_{{\rm R}\mathbf{K}} + a^\dagger_{{\rm R}\mathbf{K}}\, \mathbf{f}^*_{{\rm R}\mathbf{K}}\big], \tag{B3}$$

where the vibrational eigenfunctions $\mathbf{f}_{{\rm R}\mathbf{K}}(\mathbf{r})$ have dimensions of $L^{-\frac{3}{2}}$ and satisfy

$$\int d^3r\ \mathbf{f}^*_{{\rm R}\mathbf{K}} \cdot \mathbf{f}_{{\rm R}\mathbf{K}'} = \delta_{\mathbf{K}\mathbf{K}'}. \tag{B4}$$

Here $c_{\rm R} = \xi\, v_{\rm t}$, where ξ is the root between 0 and 1 of

$$\xi^6 - 8\xi^4 + 8(3 - 2\nu^2)\xi^2 - 16(1 - \nu^2) = 0, \tag{B5}$$

and where

$$\nu \equiv v_{\rm t}/v_{\rm l} \tag{B6}$$

is the ratio of transverse and longitudinal bulk sound velocities. For Si, $\nu = 0.69$ and $\xi = 0.88$; hence

$$c_{\rm R} = 5.2 \times 10^5\,{\rm cm\ s^{-1}}. \tag{B7}$$

The z component of the vibrational eigenfunction at the point $\mathbf{r} = 0$ on the surface is

$$f^z_{\rm R}(0) = \sqrt{\frac{2\gamma^3\eta^2|\mathbf{K}|}{(\gamma-\eta)(\gamma-\eta+2\gamma\eta^2)\mathcal{A}}}\left[1 - \left(\frac{2}{1+\eta^2}\right)\right], \tag{B8}$$

where

$$\gamma \equiv \sqrt{1-(c_{\rm R}/v_{\rm l})^2} \quad \text{and} \quad \eta \equiv \sqrt{1-(c_{\rm R}/v_{\rm t})^2}. \quad \text{(B9)}$$

We find that the Rayleigh branch contributes to the local DOS (9) an amount (for positive ω)

$$\text{R branch}: \qquad N(\omega) = \frac{g_1 \hbar \omega}{4\pi\rho c_{\rm R}^3}, \quad g_1 \approx 0.42. \quad \text{(B10)}$$

Note that g_1 generally depends on ν, the value quoted in (B10) corresponding to Si.

Next we consider the branches with continuous c. Here

$$\mathbf{u} = \sum_{\mathbf{K}} \int_\Gamma dc \, \sqrt{\frac{\hbar}{2\rho c|\mathbf{K}|}} \left[a_{m\mathbf{K}c}\, \mathbf{f}_{m\mathbf{K}c} + a^\dagger_{m\mathbf{K}c}\, \mathbf{f}^*_{m\mathbf{K}c} \right], \quad \text{(B11)}$$

where the vibrational eigenfunctions have dimensions of $L^{-\frac{3}{2}} c^{-\frac{1}{2}}$ and satisfy

$$\int d^3r \; \mathbf{f}^*_{m\mathbf{K}c} \cdot \mathbf{f}_{m'\mathbf{K}'c'} = \delta_{mm'}\, \delta_{\mathbf{K}\mathbf{K}'}\, \delta(c-c'). \quad \text{(B12)}$$

The range Γ of the c integration in (B11) is $[v_{\rm t}, \infty]$ for $m = $ SH, $[v_{\rm l}, \infty]$ for $m = \pm$, and $[v_{\rm t}, v_{\rm l}]$ for the $m = 0$ branch. The contribution to the local DOS (for $\omega \geq 0$) from these branches is given by

$$N(\omega) = \frac{\hbar}{2\rho\omega} \sum_{\mathbf{K}} \int_\Gamma dc \; |f^z_{m\mathbf{K}c}(0)|^2 \, \delta(\omega - c|\mathbf{K}|). \quad \text{(B13)}$$

The SH modes are polarized in the xy plane and therefore do not contribute to (9). The $\pm$ modes have surface amplitude

$$f^z_\pm(0) = \sqrt{\frac{|\mathbf{K}|}{4\pi c \mathcal{A}}} \left[\pm\sqrt{\alpha}\,(1 + A \pm iB) + \frac{i}{\sqrt{\beta}}(1 - A \mp iB) \right], \quad \text{(B14)}$$

where

$$A \equiv \frac{(\beta^2-1)^2 - 4\alpha\beta}{(\beta^2-1)^2 + 4\alpha\beta}, \quad \text{(B15)}$$

$$B \equiv \frac{4\sqrt{\alpha\beta}(\beta^2-1)}{(\beta^2-1)^2 + 4\alpha\beta}, \quad \text{(B16)}$$

$$\alpha \equiv \sqrt{(c/v_{\rm l})^2 - 1}, \quad \text{and} \quad \beta \equiv \sqrt{(c/v_{\rm t})^2 - 1}, \quad \text{(B17)}$$

are all real functions of c. The $m = \pm$ branches together contribute an amount

$$\pm \text{ branches}: \qquad N(\omega) = \frac{g_2 \hbar \omega}{4\pi^2 \rho v_{\rm l}^3}, \quad g_2 \approx 1.0. \quad \text{(B18)}$$

The value for g_2, obtained by doing the integration over c in Eq. (B13) numerically, is valid only for the value of ν corresponding to Si.

The $m = 0$ branch has amplitude

$$f^z_0(0) = \sqrt{\frac{|\mathbf{K}|}{2\pi c\beta\mathcal{A}}} \left[-\gamma D + i(1-E) \right], \quad \text{(B19)}$$

where

$$D \equiv \frac{4\beta(\beta^2-1)^3 - 16i\gamma\beta^2(\beta^2-1)}{(\beta^2-1)^4 + 16\gamma^2\beta^2} \quad \text{(B20)}$$

and

$$E \equiv \frac{(\beta^2-1)^4 - 16\gamma^2\beta^2 - 8i\gamma\beta(\beta^2-1)^2}{(\beta^2-1)^4 + 16\gamma^2\beta^2} \quad \text{(B21)}$$

are complex-valued functions of c. This leads to a contribution

$$0 \text{ branch}: \qquad N(\omega) = \frac{g_3 \hbar \omega}{8\pi^2 \rho v_{\rm t}^3}, \quad g_3 \approx 0.59. \quad \text{(B22)}$$

As before, g_3 is obtained numerically and assumes a value of ν valid for Si. Combining the three contributions (B10), (B18), and (B22), yields [24]

$$N(\omega) = \frac{\hbar\omega}{4\pi^2\rho} \left[\frac{g_1\pi}{c_{\rm R}^3} + \frac{g_2}{v_{\rm l}^3} + \frac{g_3}{2v_{\rm t}^3} \right]. \quad \text{(B23)}$$

Using Eq. (B23) we obtain the estimate (26).

[1] K. Schwab, E. A. Henriksen, J. M. Worlock, and M. L. Roukes, Nature **404**, 974 (2000).

[2] L. G. C. Rego and G. Kirczenow, Phys. Rev. Lett. **81**, 232 (1998).

[3] B. J. van Wees, H. van Houten, C. W. J. Beenakker, J. G. Williamson, L. P. Kouwenhoven, D. van der Marcel, and C. T. Foxen, Phys. Rev. Lett. **60**, 848 (1988).

[4] D. A. Wharama *et al.*, J. Phys. C **21**, L209 (1988).

[5] For a review see C. W. J. Beenakker and H. van Houten in *Solid State Physics: Advances in Research and Applications*, edited by H. Ehrenreich and D. Turnbull (Academic Press, San Diego, 1991), Vol. 44.

[6] M. Büttiker, in *Semiconductors and Semimetals*, edited by M. Reed (Academic Press, San Diego, 1992), Vol. 35.

[7] The Landauer formula can be applied to the case of weak tunneling provided one includes an energy-dependent transmission probability for each channel. However, these transmission probabilities would have to be calculated microscopically, which amounts to using our approach.

[8] J. R. Schrieffer, D. J. Scalapino, and J. W. Wilkins, Phys. Rev. Lett. **10**, 336 (1963).

[9] See also G. D. Mahan, *Many-Particle Physics*, 3rd ed. (Plenum Publishers, New York, 2000).

[10] D. E. Angelescu, M. C. Cross, and M. L. Roukes, Superlattices Microstruct. **23**, 673 (1998).
[11] W. A. Little, Can. J. Phys. **37**, 334 (1959).
[12] F. W. Sheard and G. A. Toombs, J. Phys. C **5**, L166 (1972).
[13] M. C. Cross and R. Lifshitz, cond-mat/0011501.
[14] L. W. Molenkamp, Th. Gravier, H. van Houten, O. J. A. Buijk, M. A. A. Mabesoone, and C. T. Foxen, Phys. Rev. Lett. **68**, 3765 (1992).
[15] C. L. Kane and M. P. A. Fisher, Phys. Rev. B **55**, 15832 (1997).
[16] C. L. Kane and M. P. A. Fisher, Phys. Rev. Lett. **76**, 3192 (1996).
[17] Note that $\int_0^\infty dx\, x^4 e^x (e^x-1)^{-2} = 4\pi^4/15$.
[18] *Semiconductors: Group IV Elements and III-V Compounds*, edited by O. Madelung (Springer-Verlag, Berlin, 1991).
[19] W. Fulkerson, J. P. Moore, R. K. Williams, R. S. Graves, and D. L. McElroy, Phys. Rev. **167**, 765 (1968).
[20] C. J. Glassbrenner and G. A. Slack, Phys. Rev. **134**, A1058 (1964).
[21] This is correct only at the low energies of interest in the present work. At higher energies it is of course possible to have forbidden regions, for example, in a vibrational analog of a photonic band-gap structure, or simply at energies higher than the acoustic and optical phonon bands of an ordinary crystal.
[22] H. Ezawa, Ann. Phys. **67**, 438 (1971).
[23] Here 'R' denotes the Rayleigh branch.
[24] It is useful to compare this result with the corresponding *bulk* spectral density of an isotropic elastic continuum, calculated with periodic boundary conditions,

$$N_{\rm bulk}(\omega) = \frac{\hbar\omega}{4\pi^2\rho}\left(\frac{1}{v_{\rm l}^3}+\frac{2}{v_{\rm t}^3}\right).$$